COMMUNICATION

ChemComm
www.rsc.org/chemcomm

$CsPb_3Bi_3Te_8$ and $CsPb_4Bi_3Te_9$: low-dimensional compounds and the homologous series $CsPb_mBi_3Te_{5+m}$

Kuei-Fang Hsu,[a] Sangeeta Lal,[b] Tim Hogan[b] and Mercouri G. Kanatzidis*[a]

[a] *Department of Chemistry and Center for Fundamental Materials Research, Michigan State University, East Lansing, MI 48824, USA. E-mail: kanatzid@cem.msu.edu*

[b] *Department of Electrical and Computer Engineering, Michigan State University, East Lansing, MI 48824, USA. E-mail: hogant@egr.msu.edu*

Received (in Cambridge, UK) 28th February 2002, Accepted 30th April 2002
First published as an Advance Article on the web 24th May 2002

Two new thermoelectric materials of quaternary bismuth telluride $CsPb_3Bi_3Te_8$ and $CsPb_4Bi_3Te_9$ are reported, which are members of a homologous series featuring anionic slabs $[Pb_mBi_3Te_{5+m}]^-$ (m = 1–4) of monotonically increasing thickness.

Research in new thermoelectric materials is focused on heavily doped semiconductors composed of atoms with large mass, complex crystal structures and narrow band-gap.[1] These attributes can lead to high power factors and low thermal conductivity both necessary to achieve a high figure of merit.[2–7] Recently, we reported the phase $CsBi_4Te_6$, which when properly doped can reach a high thermoelectric figure of merit below room temperature.[8] In an effort to produce new materials that resemble $CsBi_4Te_6$, we introduced Pb metal into its layered framework and searched for corresponding quaternary phases. This produced $CsPbBi_3Te_6$ and $CsPb_2Bi_3Te_7$, which featured layered structures with infinite anionic 'PbTe'-type slabs of $[PbBi_3Te_6]^-$ and $[Pb_2Bi_3Te_7]^-$ separated with Cs^+ cations.[9] To our surprise we subsequently discovered that reactions of $CsBi_4Te_6$ with larger amounts of PbTe continued to form more interesting higher order phases (rather than mixtures of $CsPb_2Bi_3Te_7$ and PbTe) in such a fashion that we can now define a new homologous series of the type $CsPb_mBi_3Te_{5+m}$ with systematically varying structure and composition. The new family defines a new structural motif that can be exploited in designing future thermoelectrically promising materials. The two higher order phases $CsPb_3Bi_3Te_8$ (m = 3) and $CsPb_4Bi_3Te_9$ (m = 4) are characterized by enlarged slab thickness and a robust framework that is based on the NaCl motif.†

The structure of $CsPb_3Bi_3Te_8$ features thick $[Pb_3Bi_3Te_8]^-$ slabs separated by layers of Cs^+ cations perpendicular to the b axis. The $[Pb_3Bi_3Te_8]^-$ slab consists of three distinct M metal sites occupied by both Bi^{3+} and Pb^{2+} ions[10] and it can be viewed as a fragment excised from PbTe-type structure with a thickness of eight {PbTe} monolayers, see Fig. 1Ac.

Reacting $CsBi_4Te_6$ with an extra equivalent of PbTe led to the next member $CsPb_4Bi_3Te_9$, which also adopts a layered structure made up of even thicker $[Pb_4Bi_3Te_9]^-$ slabs (Fig. 1Ad). As indicated by bond-valence sum calculations, both Bi^{3+} and Pb^{2+} ions occupy the five distinct M sites in the $[Pb_4Bi_3Te_9]^-$ slab.[10] The slab (also a NaCl slice) is expanded by one {MTe} monolayer compared to the $[Pb_3Bi_3Te_8]^-$ slab, Fig. 1B. The M metals sites in $[Pb_3Bi_3Te_8]^-$ and $[Pb_4Bi_3Te_9]^-$ are octahedrally coordinated with Te atoms and posses slight local distortions. Interestingly, the MTe_6 octahedra present in the strucrures increase their distortions from the interior to the exterior of the slabs.[11] This may result from relaxation effects since the Te atoms are coordinated with 6, 4 and 2 M atoms as one moves from the center of the slab towards the surface.

The two layered compounds reported here along with $CsPbBi_3Te_6$ and $CsPb_2Bi_3Te_7$ clearly establish the brand-new homologous series $CsPb_mBi_3Te_{5+m}$ (m = 1, 2, 3, 4). These phases crystallize in the same space group and have systematically varying structures, see Table 1 and Fig. 1.[12] The thickness difference between the $[Pb_4Bi_3Te_9]^-$ and $[Pb_3Bi_3Te_8]^-$ slabs is 2.252 Å, *i.e.* the thickness of one {MTe} monolayer, which corresponds to half the value of dimensional difference of the b axes between sequential structures, 4.401 Å.[13]

Occupancy refinements showed that the Cs sites were not fully occupied. The occupancies were 0.93 for $CsPb_3Bi_3Te_8$ and 0.96 for $CsPb_4Bi_3Te_9$. The final formulae were thus adjusted to be Bi-rich compositions for electroneutrality, *i.e.*

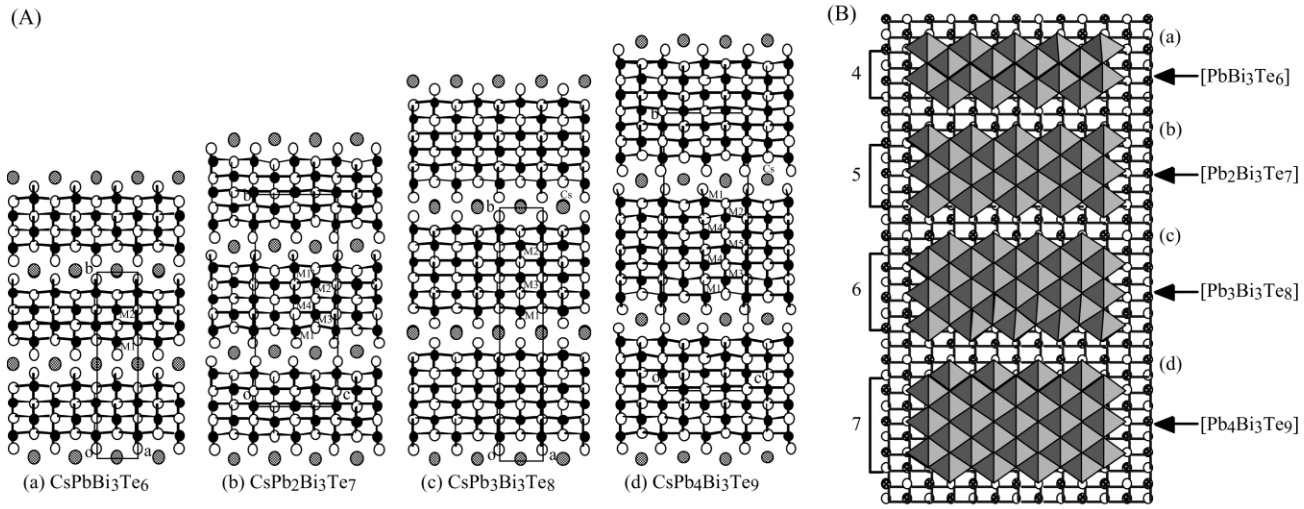

Fig. 1 (A) The structures of (a) $CsPbBi_3Te_6$, (b) $CsPb_2Bi_3Te_7$, (c) $CsPb_3Bi_3Te_8$ and (d) $CsPb_4Bi_3Te_9$ in projection down the c axis for (a) and (c) and the a axis for (b) and (d). The largest shaded circles are Cs atoms, medium shaded circles are M atoms and open circles are Te atoms. (B) A perspective view of the PbTe structure along the [011] direction and slices thereof. The polyhedra represent $PbTe_6$ octahedra. The $[PbBi_3Te_6]^-$, $[Pb_2Bi_3Te_7]^-$, $[Pb_3Bi_3Te_8]^-$ and $[Pb_4Bi_3Te_9]^-$ slabs are fragments excised from this lattice with (a) 4, (b) 5, (c) 6, and (d) 7 monolayers. Crystals of these phases grow as long thin needles with the needle direction being parallel to the projection view shown here.

DOI: 10.1039/b202043b

Table 1 Summary of crystallographic data for the layered compounds $CsPb_mBi_3Te_{5+m}$

m	Space group	*a*/Å	*b*/Å	*c*/Å	*Z*	*V*/Å^3	*N*[a]
1	*Cmcm*	6.3326(6)	28.667(3)	4.3637(4)	4	792.1(2)	4
2	*Cmcm*	4.3456(6)	32.476(5)	12.508(2)	8	1765.2(7)	5
3	*Cmcm*	6.3736(8)	37.731(5)	4.4416(6)	4	1068.1(4)	6
4	*Cmcm*	4.4524(6)	42.132(6)	12.742(2)	8	2390.3(9)	7

[a] *N* is the number of monolayers in each slab.

$Cs_{0.93}Pb_{2.93}Bi_{3.07}Te_8$ and $Cs_{0.96}Pb_{3.96}Bi_{3.04}Te_9$. These were confirmed with microprobe energy dispersive analyses. Interestingly, the Cs atom occupation approaches the ideal value of 1 with increasing *m* value (*i.e.* slab thickness). The Cs cations are coordinated with nine Te atoms distributed peripherally around the slabs in the four structures. The topography of even-layered (*i.e.* $m = 1, 3$) slabs is different from that of odd-layered (*i.e.* $m = 2, 4$) slabs where the terminal μ_2-Te atoms are arranged in a staggered fashion in the former, and in an eclipsed fashion in the latter. However, these slabs stack along the *b* axis by *c*-glide symmetry so that they generate tricapped trigonal pyrismatic sides for the Cs atoms. Because the rows of terminal μ_2-Te atoms found on the slab surfaces shift from being on *m*2*m* sites in $[Pb_mBi_3Te_{5+m}]^-$ ($m = 1, 3$) to being on *m* sites in $[Pb_mBi_3Te_{5+m}]^-$ with ($m = 2, 4$), the repeating units along the *c*-axis of $CsPb_mBi_3Te_{5+m}$ with $m = 2$ and 4 are doubled compared to those with $m = 1$ and 3.

Charge transport measurements on oriented polycrystalline ingots of $CsPb_mBi_3Te_{5+m}$ ($m = 3, 4$) parallel to the needle direction show metal-like behavior in the electrical conductivity, which increases as the temperature drops. As shown in Fig. 2, the electrical conductivities decreases from 500 S cm^{-1} at 80 K to 410 S cm^{-1} at 350 K for $CsPb_3Bi_3Te_8$ and from 460 S cm^{-1} at 80 K to 400 S cm^{-1} at 350 K for $CsPb_4Bi_3Te_9$. The thermopower values are between -50 and -70 μV K^{-1} at 350 K. The moderate thermopower and metallic like temperature dependence of conductivity indicate that $CsPb_mBi_3Te_{5+m}$ materials are heavily doped. This is consistent with their Bi-rich non-stoichiometric nature. Remarkably, the thermal conductivity at room temperature is very low at ~1.5 W m^{-1} K^{-1} for both $CsPb_3Bi_3Te_8$ and $CsPb_4Bi_3Te_9$ and lower than Bi_2Te_3 (~1.8 W m^{-1} K^{-1}) the premier thermoelectric material. The long lattice period, two-dimensional crystal structures and heavy atoms in the structure play an important role in depressing the thermal conductivities in these materials.

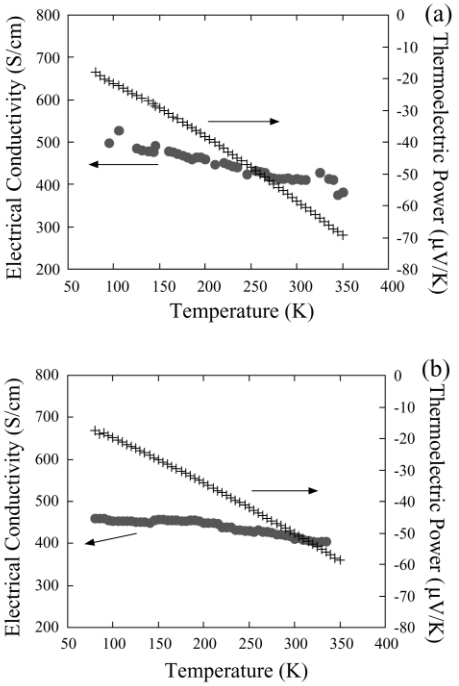

Fig. 2 Electrical conductivity and thermopower data for oriented polycrystalline ingot samples of (a) $CsPb_3Bi_3Te_8$ and (b) $CsPb_4Bi_3Te_9$. The crosses are thermopower and circles are electrical conductivity.

Financial support from the Office of Naval Research and DARPA is gratefully acknowledged.

Notes and references

† Crystals of $CsPb_mBi_3Te_{5+m}$ ($m = 3, 4$) were obtained by reacting $CsBi_4Te_6$ with PbTe in molar ratios of 1:4 and 1:6, respectively. Single phase of $CsPb_3Bi_3Te_8$ was also obtained by reacting Cs metal and $Pb_{2.85}Bi_3Te_8$ with molar ratio 0.85:1. Single phase of $CsPb_4Bi_3Te_9$ was obtained by reacting Cs metal and $Pb_{3.9}Bi_3Te_9$ with molar ratio 0.9:1. The two reactions were heated at 700 °C for 2 h followed by cooling to 500 °C in 2 h and finally quenching to room temperature.

Crystal data: $Cs_{0.93}Pb_{2.93}Bi_{3.07}Te_8$, orthorhombic, *Cmcm*, $a = 6.3736(8)$, $b = 37.731(5)$, $c = 4.4416(6)$ Å, $V = 1068.1(4)$ Å^3, $Z = 4$, $D_c = 15.765$ g cm^{-3}, $\mu = 124.459$ mm^{-1}, total reflections 3069, independent reflections 757 ($R_{int} = 0.0588$), $R1 = 0.0597$, $wR2 = 0.1583$. $Cs_{0.96}Pb_{3.96}Bi_{3.04}Te_9$, orthorhombic, *Cmcm*, $a = 4.4524(6)$, $b = 42.133(6)$, $c = 12.742(2)$ Å, $V = 2390.3(6)$ Å^3, $Z = 8$, $D_c = 15.23$ g cm^{-3}, $\mu = 125.92$ mm^{-1}, total reflections 7600, independent reflections 1727 ($R_{int} = 0.075$), $R1 = 0.049$, $wR2 = 0.107$. CCDC reference numbers 180732 and 180733. See http://www.rsc.org/suppdata/cc/b2/b202043b/ for crystallographic data in CIF or other electronic format.

1 G. A. Slack, New Materials and Performance Limits for Thermoelectric Cooling. In *CRC Handbook of Thermoelectrics*, ed. D. M. Rowe, CRC Press, Boca Raton, FL, 1995, pp. 407–440.
2 A. Mrotzek, L. Iordanidis and M. G. Kanatzidis, *Chem. Commun.*, 2001, **17**, 1648–1649.
3 L. Iordanidis, P. W. Brazis, T. Kyratsi, J. Ireland, M. Lane, C. R. Kannewurf, W. Chen, J. S. Dyck, C. Uher, N. A. Ghelani, T. Hogan and M. G. Kanatzidis, *Chem. Mater.*, 2001, **13**, 622–633.
4 K. S. Choi, D. Y. Chung, A. Mrotzek, P. Brazis, C. R. Kannewurf, C. Uher, W. Chen, T. Hogan and M. G. Kanatzidis, *Chem. Mater.*, 2001, **13**, 756–764.
5 A. Mrotzek, D. Y. Chung, N. A. Ghelani, T. Hogan and M. G. Kanatzidis, *Chem. Eur, J.*, 2001, **7**, 1915–1926.
6 Y. C. Wang and F. J. DiSalvo, *Chem. Mater.*, 2000, **12**, 1011–1017.
7 D. Y. Chung, L. Iordanidis, K. K. Rangan, P. W. Brazis, C. R. Kannewurf and M. G. Kanatzidis, *Chem. Mater.*, 1999, **11**, 1352–1362.
8 D. Y. Chung, T. Hogan, P. W. Brazis, M. Rocci-Lane, C. R. Kannewurf, M. Bastea, C. Uher and M. G. Kanatzidis, *Science*, 2000, **287**, 1024–1027.
9 K. F. Hsu, D. Y. Chung, S. Lal, A. Mrotzek, T. Kyratsi, T. Hogan and M. G. Kanatzidis, *J. Am. Chem. Soc.*, 2002, 000asap. article.
10 The metal sites are assumed to be Pb atoms and bond valence $s = \exp[(R_o - R_i)/B]$ where $R_o = 2.873$, $B = 0.37$ and R_i is the bond length. The sums of bond valence were 2.85, 2.55, 2.54 for M(1), M(2) and M(3) metal sites in $CsPb_3Bi_3Te_8$, respectively. The sums of bond valence were 2.83, 2.39, 2.74, 2.52, 2.53 for M(1), M(2), M(3), M(4) and M(5) metal sites in $CsPb_4Bi_3Te_9$, respectively: I. D. Brown, *J. Appl. Crystallogr.*, 1996, **29**, 479–480.
11 Distortions of octahedra 10^4 are 29.8, 10.0 and 0.3 for $M(1)Te_6$, $M(2)Te_6$ and $M(3)Te_6$ in $CsPb_3Bi_3Te_8$, respectively. Distortions of octahedra are 30.4, 10.6, 10.0, 2.7 and 0.1 for $M(1)Te_6$, $M(2)Te_6$, $M(3)Te_6$, $M(4)Te_6$ and $M(5)Te_6$ in $CsPb_4Bi_3Te_9$, respectively. M(1), M(2), M(3), M(4) and M(5) are metal sites situated from the inner to the outer sphere of slabs (an octahedral distortion is defined by $= 1/6\Sigma[(R_i - R_a)/R_a]^2$ where R_i is the bond length and R_a is the average bond length).
12 The *b* axis of the $CsPb_mBi_3Te_{5+m}$ ($m = 1, 2, 3$ and 4) structures evolves linearly with the number of {MTe} monolayers in the slabs *N* ($N = 4$, 5, 6 and 7) according to the equation $y = 10.144 + 4.565x$, $R^2 = 0.997$.
13 The thickness difference between the $[Pb_3Bi_3Te_8]^-$ and $[Pb_2Bi_3Te_7]^-$ slabs, 2.574 Å, is half the value of the dimensional difference of *b* axes between sequential structures, 5.255 Å.